

We are IntechOpen, the world's leading publisher of Open Access books Built by scientists, for scientists

6,900

Open access books available

186,000

International authors and editors

200M

Downloads

Our authors are among the

154

Countries delivered to

TOP 1%

most cited scientists

12.2%

Contributors from top 500 universities



WEB OF SCIENCE™

Selection of our books indexed in the Book Citation Index
in Web of Science™ Core Collection (BKCI)

Interested in publishing with us?
Contact book.department@intechopen.com

Numbers displayed above are based on latest data collected.
For more information visit www.intechopen.com



Defect Structure Versus Superconductivity in MeB₂ Compounds (Me = Refractory Metals) and One-Dimensional Superconductors

A.J.S. Machado, S.T. Renosto, C.A.M. dos Santos, L.M.S. Alves and Z. Fisk

Additional information is available at the end of the chapter

<http://dx.doi.org/10.5772/48625>

1. Introduction

More than 24,000 inorganic phases are known. Of these phases approximately 16,000 are binary or pseudobinary while about 8,000 are ternary or pseudo-ternary. However, it is surprising to note that the observation of superconductivity in these alloys is a rare phenomenon. Superconductivity is ubiquitous but sparsely distributed and can be considered a rare phenomenon among the known alloys. BCS theory has been enormously successful in explaining the superconducting phenomena from the microscopic view point. The fundamental idea of this theory is the formation of Cooper pairs of electrons, mediated by phonons, the quantum of vibration of the crystal lattice [1]. Thus maximizing the critical temperature is involved with maximizing the electron-phonons coupling. Among the intermetallic materials, the binary cubic (A₃B) so-called A15 compounds displayed the highest T_c, until the discovery of superconducting cuprates. Among these materials in particular, Nb₃Sn and V₃Si with critical temperatures of 18.0 K and 17.1 K respectively have lattice instabilities of martensitic-type occurring at temperatures T_m very close to the maximum T_c. In the phase diagram of T_m and T_c versus Pressure (P) of V₃Si, the martensitic phase line intersects and stops exactly at the superconducting phase boundary. A qualitative example of this kind of the behavior can be observed in the Figure 1. Data exists beyond the extrapolated intersection shown and finds that there is no martensitic distortion occurring below T_c in this pressure regime. One way to think about this behavior is in terms of a lattice softening arising from strong electron-phonon coupling. Both the martensitic distortion and superconductivity arise from this coupling, and when the superconductivity T_c occurs at higher temperature than that of the lattice distortion, the energy gap that opens in the superconducting state gaps out at the same time phonon fluctuations that give rise to the lattice distortion [2-3]. One has, then, two phases that are competing for the same resource.

A similar type behavior is observed in heavy Fermion (HF) superconducting materials. Here antiferromagnetic order competes with the superconducting transition, both phases arising from electronic coupling to magnetic fluctuation in the heavy electron liquid.

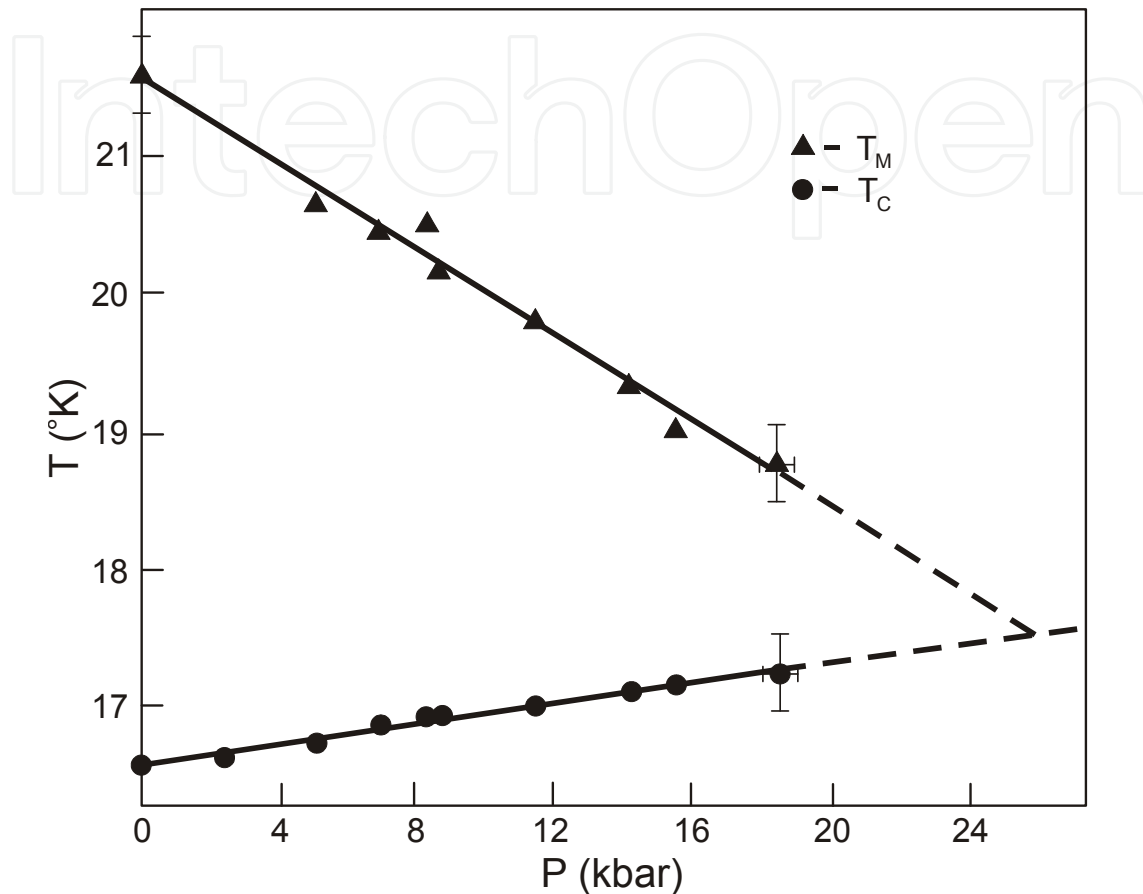


Figure 1. Schematic representation of the temperature dependence with pressure showing the critical temperature and martensitic temperature for V_3Si .

With the heavy Fermions, all superconductors are found in the vicinity of a quantum critical point, where the antiferromagnetic order has been driven to zero Kelvin ($T = 0K$). The general characteristics of high critical temperature cuprates are often discussed in terms of the kind of phase diagram found in the HF materials. A line known as the pseudogap intersects the maximum T_c in a superconducting dome in the temperature control parameter phase diagram, in general doping level being the control parameter [3]. There continues debate as to whether the pseudogap line represents a true phase transition. However, it is arguably the temperature setting the critical superconducting transition temperature upper limit. Again, the similarities with other instabilities discussed here are evident, with the temperature of the pseudogap intercepting the maximum of T_c against a control parameter that in this case is the doping level. This same discussion is also relevant to recent Fe-based pnictide superconductors. In this set of materials two competing phases are observed in the phase diagram, the non-superconducting one a structural instability or an SDW. Their

transition temperatures intersect the superconducting transition temperature curve in the phase diagram versus pressure and/or composition. At the pressure suppressing the structural or SDW transition down to the superconducting T_c superconductivity does not appear to coexist with the SDW or structurally distorted phase. However, the data are not sufficient to say that the critical temperature of the superconducting transition is maximized at the intercept of the SDW transition, but the results seem to suggest that this may occur. In addition, the organic superconductors show similar behavior to that which occurs in high critical temperature cuprates. In all these cases maximizing the superconducting temperature appears to involve suppressing a secondary phase which competes with the phenomenon of superconductivity, whether CDW, SDW, T_m or other competitive instability. These experiments all suggest that superconducting pairs are utilizing the same fluctuation spectrum that supports the order of the phases it competes with. The key to superconductivity is to be found in frustrating the competing order so that the superconducting instability of the Fermi surface can gap out parts of the fluctuation spectrum favoring the second phase. Even in one-dimensional systems instabilities play a role in the superconducting behavior [4-5]. The superconducting critical temperature increases upon applying hydrostatic pressure while simultaneously suppressing the electronic CDW. Within this general scenario is the superconductivity of compounds which can crystallize in AlB₂ prototype structure. Our discussion of superconductivity in this structure-type is based on the defect structures that these compounds may have.

1.1. Superconductivity in compounds with AlB₂ prototype structure

The first superconductor found to crystallize in the AlB₂ prototype structure was discovered by A. S. Cooper et. al. [6] In this paper the authors showed that NbB₂ as well MoB₂ can exhibit superconductivity. However, stoichiometric NbB₂ was not superconducting, but adding excess boron for a nominal composition of NbB_{2.5} yielded bulk superconductivity observed at 3.87 K, determined from the measurement of the specific heat. In the same article the authors discussed the high temperature phase MoB₂. When a nominal composition MoB_{2.5} was splat-melted forcing excess boron into lattice the material had a superconducting transition close to 7.45 K. These results were not confirmed by other authors and remained of little interest to the scientific community until the discovery of superconductivity in MgB₂ with critical temperature close to 40.0 K [7]. In the Nb-B system the NbB₂ phase shows a wide range of boron stoichiometry where a defect structure can explain this large range of solubility. Recently C. A. Nunes et. al. [8] made a systematic study of the B-solubility in NbB₂. The homogeneity of the phases obtained was determined by neutron diffraction and a maximum critical temperature was found to be 3.9 K. This study raises anew the question of the nature of defects that can be generated in these compounds. The stability of the phase NbB₂ spans a wide range of composition as shown in the diagram in Figure 2.

At the solubility limit the Nb-B inter-atomic distance in NbB₂ phase is constant. This indicates that variations in lattice parameters "a" and "c" inside of the stability range do not occur randomly but are such as to maintain a constant Nb-B distance of 2.43Å. To explain the wide

stability range of the NbB₂ phase, some authors propose a superstructure of defect vacancies in the crystal lattice [10]. This defect structure is based on the cohesive forces in layers exerted by expansive forces in the Nb layers. Certainly this defect structure strongly influences the electronic structure, making it highly dependent on stoichiometry. The MoB₂ compound was also revisited for L. E. Muzzy et al. in [11] which reported a systematic study of the substitution of Mo by Zr in the (Mo_{0.96}Zr_{0.04})_{0.88}B₂ where the AlB₂ structure is stabilized and superconductivity can exist in the range of critical temperature between 5.9 and 8.2 K. In this case the authors claim that the superconductivity is strongly dependent on a specific defect structure such as occurs in NbB₂ compound. Another interesting compound that presents a relatively high superconducting critical temperature is CaSi₂. The equilibrium phase is hexagonal with space group R-3mh. However when this compound is submitted to the high pressure 15 GPa, an allotropic transformation occur into the AlB₂ prototype structure with sp² graphite-like planes, with superconducting critical temperature close to 14.0 K [12].

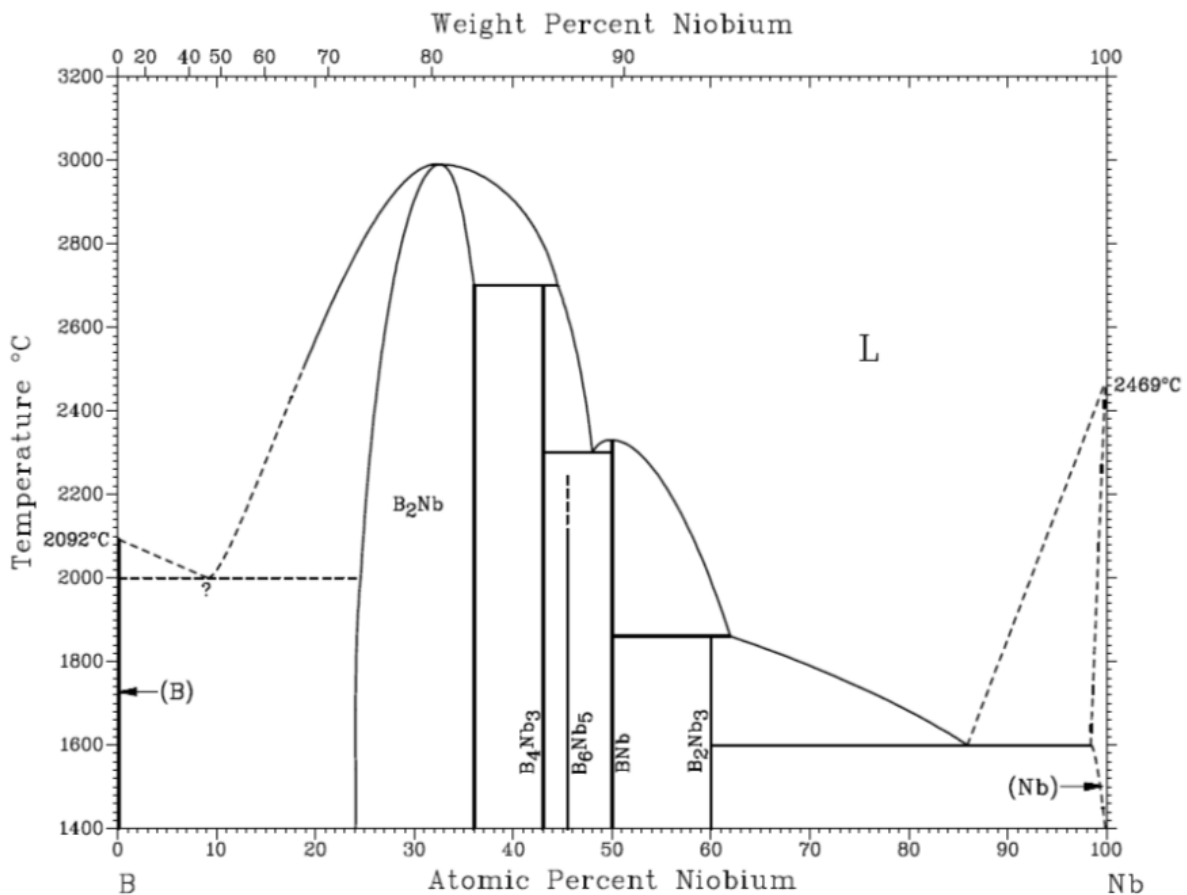


Figure 2. Phase diagram of the Nb – B system which show the wide solubility range of the NbB₂ phase. Adapted from reference [9].

Within this context we will discuss an example where an extremely stressed lattice of AlB₂ prototype yields superconductivity while the matrix compound is non-superconducting.

1.1.1. Superconductivity in a supersaturated solid solution of Zr_{1-x}V_xB₂

Since the discovery of superconductivity in MgB₂ with superconducting critical temperature close to 40 K, MB₂ materials (M = Transition Metal) with the same prototype structure as MgB₂ are considered as candidates for multiband superconductivity. As mentioned above, superconductivity in this class of material is relatively rare. Theoretical articles in the literature suggest that some member compounds are good candidates to exhibit high superconducting critical temperature. Among the suggested compounds are AuB₂, AgB₂, LiB₂, ZnB₂ and CaB₂ [13-17]. However, these theoretical predictions have not been confirmed and some of the suggested compounds do not exist in the equilibrium phase diagram. As example we mention ZnB₂ that does not exist in the Zn-B binary system in thermodynamic equilibrium. In the binary system (Zn-B) system no solubility exists between Zn and boron atoms and no intermetallic phase is observed. In our opinion the most important criterion for superconductivity in the AlB₂-type structure is defect creation such as occurs in NbB₂. Superconductivity was reported in ZrB₂ with superconducting critical temperature close to 5.5 K [18]. However, this surprising result was not confirmed by other groups. In fact single crystals of this compound (ZrB₂) are not superconducting [19]. This apparent paradox can be attributed to the possible existence of ZrB₁₂ as contaminant in the sample prepared by Gasparov et. al. [18]. A careful analysis of the Zr-B phase diagram suggests that this kind of the contamination is quite possible, ZrB₁₂ is a superconductor known for a long time, with superconducting critical temperature 5.94 K [20]. ZrB₂ also was studied at high pressure (50 Gpa) and superconductivity was not observed [21].

In order to address this problem we made a systematic study of ZrB₂ where Zr is substituted for V in VB₂ and V for Zr in ZrB₂. In both the Zr-B and V-B systems the AlB₂ structure exists and a solid solution is possible. We prepared Zr_{1-x}V_xB₂ compositions with x for 0.01 ≤ x ≤ 0.1. All the samples were prepared by arc-melting together the high purity elements taken in the appropriate amounts in a Ti gettered arc furnace on a water-cooled Cu hearth under high purity argon. The samples were remelted five times to ensure good homogeneity. Due to the low vapor pressure of these constituent elements at their melting temperatures, the weight losses during arc melting were negligible (< 0.5%). The samples were characterized by x-ray diffraction with CuK_α radiation. The results of x-ray diffractometry are shown in Figure 3.

All peaks can be indexed as belonging to AlB₂ prototype structure until x = 0.05 V content. For composition with x > 0.05, a segregation of secondary phase is observed, this secondary phase being interpreted as VB. These results indicate that the solubility limit is low. The lattice parameter as a function of V content is shown in Figure 4.

A small but consistent variation is observed indicating that the “c” lattice parameter systematically decreases with the substitution of Zr for V. However, the “a” lattice parameter is essentially constant as a function of V content. These results are consistent with the radius of V relative to Zr and indicates that V occupies the positions (0,0,0). The substitution of Zr for V yields a contraction in the Zr layers in the AlB₂ prototype structure. Indeed VB₂ presents a ~ 3.0 Å and c ~ 3.05 Å, while ZrB₂ has a ~ 3.16 Å and c ~ 3.53 Å. Thus the difference between both lattices parameters is about 5% relative to the “a” parameter

and about 16% relative to the “c” parameter. These differences explain the larger variation of the “c” lattice parameter than “a” lattice parameter shown in Figure 4. The contraction in the crystalline structure occurs until $x \sim 0.05$ in the global composition indicating that the solubility limit is quite limited. This suggests that the integrity of unit cell strongly affects the electronic structure in this material and may change radically the electronic properties in the matrix compound (ZrB_2). The magnetization dependence with temperature is shown in Figure 5 in which a superconducting transition emerges even at very low substitution of Zr by V at 6.4 K ($x=0.01$).

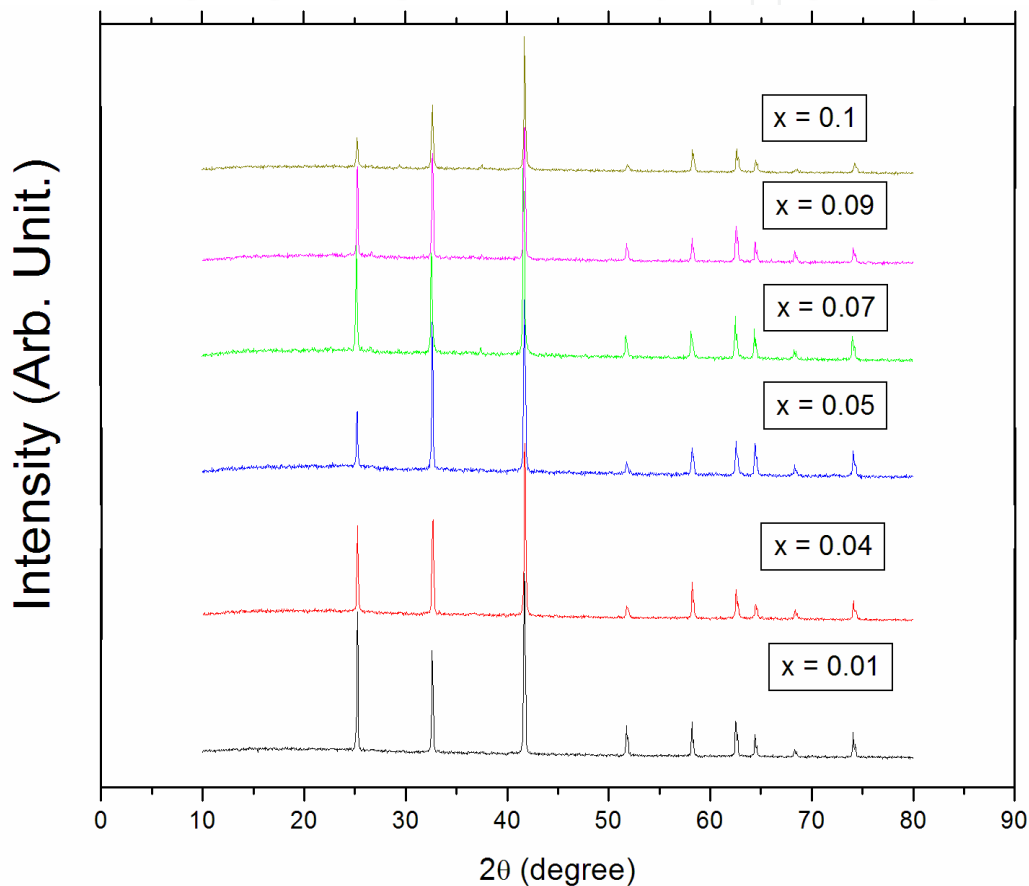


Figure 3. X-ray sequence of the samples with $0.01 \leq x \leq 0.1$ interval of composition in $\text{Zr}_{1-x}\text{V}_x\text{B}_2$.

In the inset the characteristic type II superconducting behavior is seen. These results are especially interesting because they suggest that the isoelectronic V can radically affect the electronic structure and is able to induce superconductivity in a non-superconducting matrix (ZrB_2). Indeed for the composition with $x = 0.04$ the superconducting critical temperature reaches the maximum value close to 8.52K. The dependence of magnetization with the temperature and applied magnetic field at 2.0K is shown in Figure 6. Once again clear superconducting behavior is observed close to 8.52K and the inset again reveals the type II superconducting behavior.

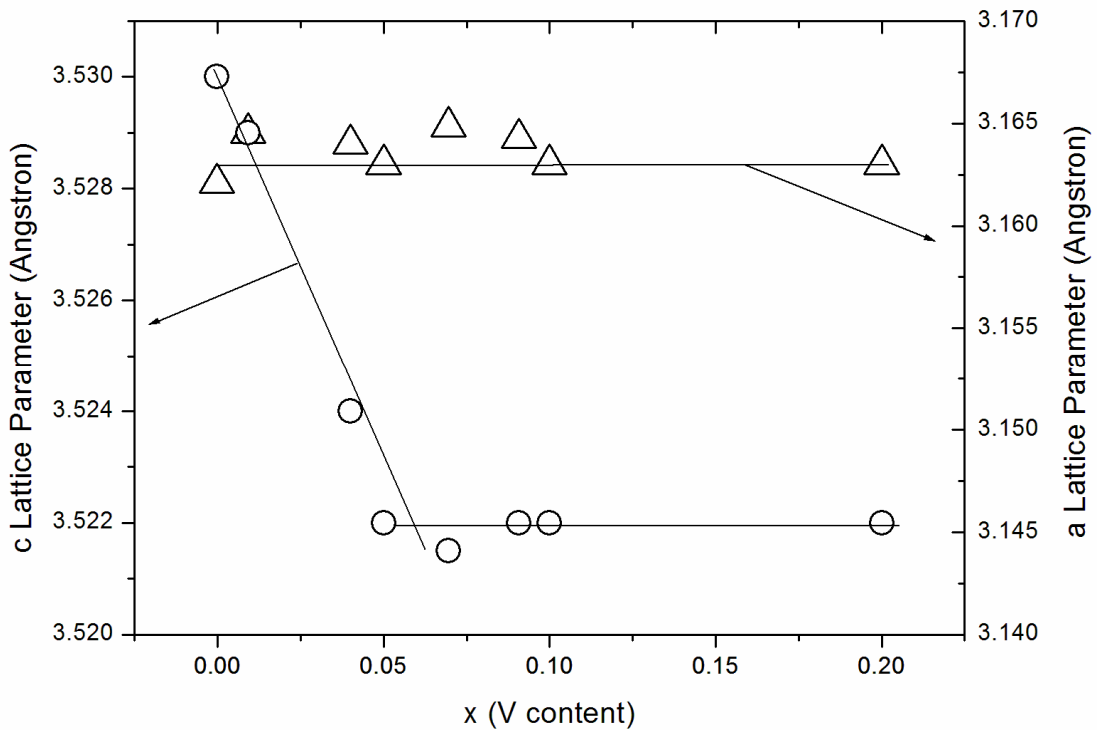


Figure 4. Lattice parameter variation as a function of vanadium content. The c lattice parameter displays a small and consistent variation with vanadium content. The a lattice parameter is essentially constant.

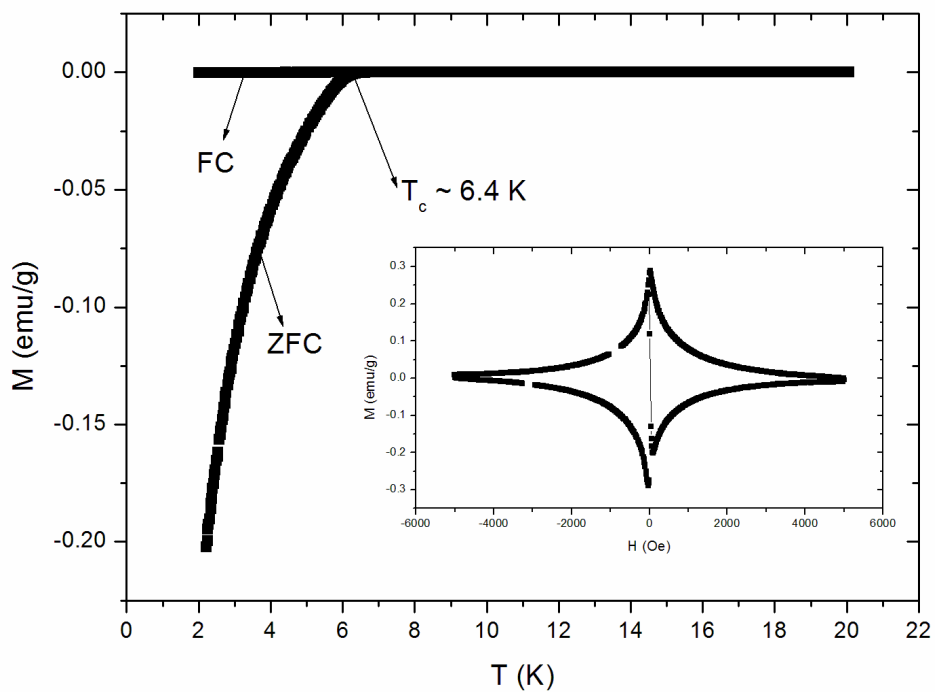


Figure 5. M vs T behavior which shows the critical temperature close to 6.4 K. The inset shows typical type II superconducting behavior.

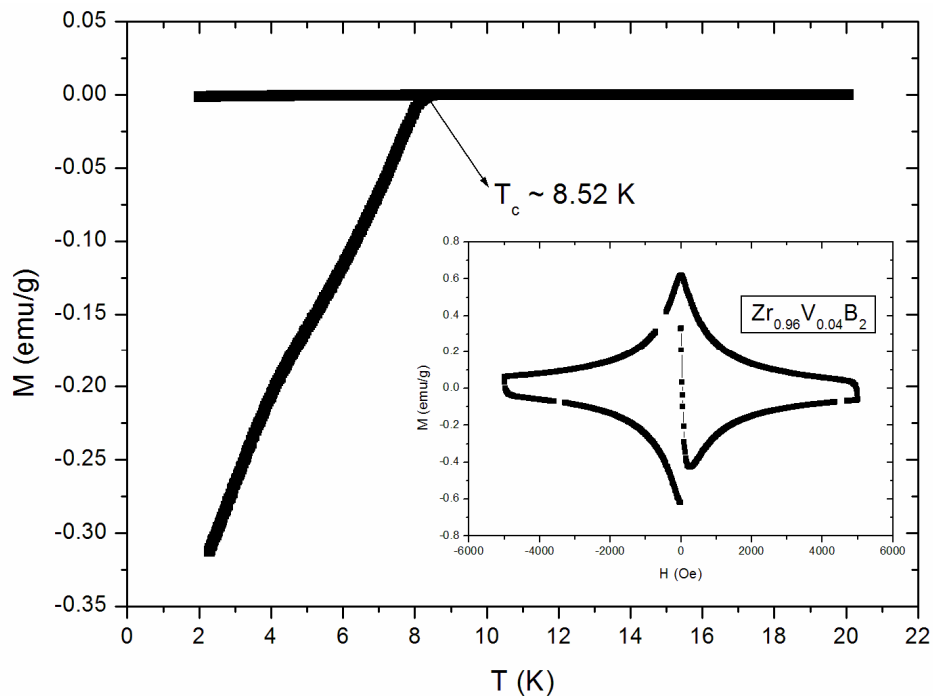


Figure 6. M vs T behavior which shows the critical temperature close to 8.52K. The inset shows typical type II superconducting behavior.

For compositions higher than $x = 0.04$ the critical temperature reaches a saturation value consistent with the solubility limit. For example, for a sample with composition $Zr_{0.95}V_{0.05}B_2$ the critical temperature is close to 8.2K as shown in Figure 7 where the dependence of the critical temperature as a function of V content is shown up to the solubility limit.

In samples with composition higher than $x = 0.05$ the critical temperature remains at 8.2K. Although the critical temperature does not change with higher V content, a decrease of the superconductor fraction is observed which is consistent with the appearance of a secondary phase.

This behavior is consistent with the solubility limit shown in Figure 4. The superconducting fraction estimate from figure 6 is about 45% of total volume of the sample indicating bulk superconductivity. The resistive behavior is shown in figure 8 where the superconducting critical temperature is consistent with the magnetization measurement shown in figure 6. The inset shows the resistivity behavior in applied magnetic field for $0 \leq \mu_0 H \leq 6.0$ T. These results suggest that the upper critical field is very high since even with applied magnetic field of $\mu_0 H = 6.0$ T the material is superconducting with critical temperature close to 6.9 K. Using the onset critical temperature it is possible to make an estimative of the upper critical field using the WHH formula [22] in the limit of short electronic mean-free path (dirty limit) given by:

$$\mu_0 H_{c2}(0) = -0.693 T_c \left(\frac{dH_{c2}}{dT} \right)_{T=T_c}. \quad (1)$$

Using this formula the upper critical field at zero Kelvin is estimated to be $\mu_0 H_{c2}(0) \sim 17.9$ T, a surprisingly high upper critical field for this class of the material. Figure 9 shows the solid

line expected in the WHH model, which fits the data very well and leads to the $\mu_0 H_{c2}(0)$ value of 17.9 T. Hence, pair breaking in this compound ($Zr_{0.96}V_{0.04}B_2$) is probably caused by orbital fields.

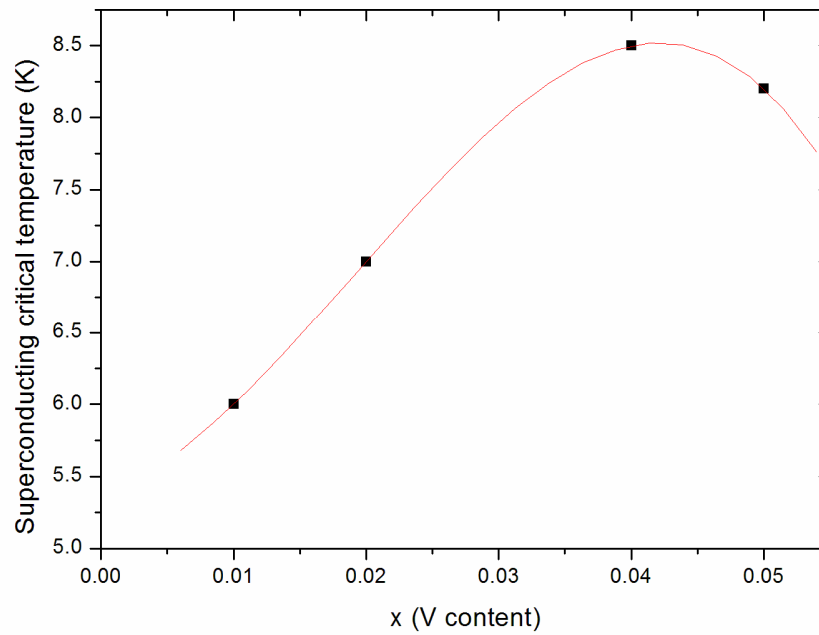


Figure 7. Superconducting critical temperature as a function of vanadium content.

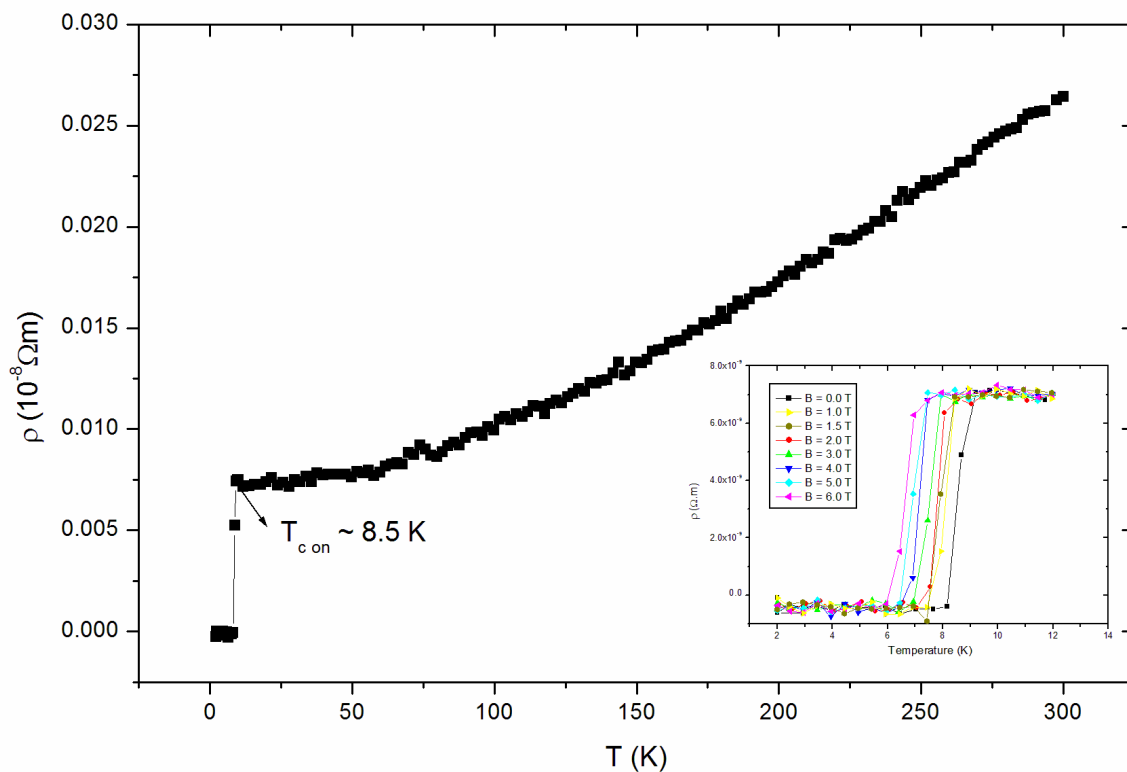


Figure 8. Resistivity as a function of temperature showing essentially the same critical temperature seen in M vs T . The inset shows the dependence of the critical temperature on applied magnetic field.

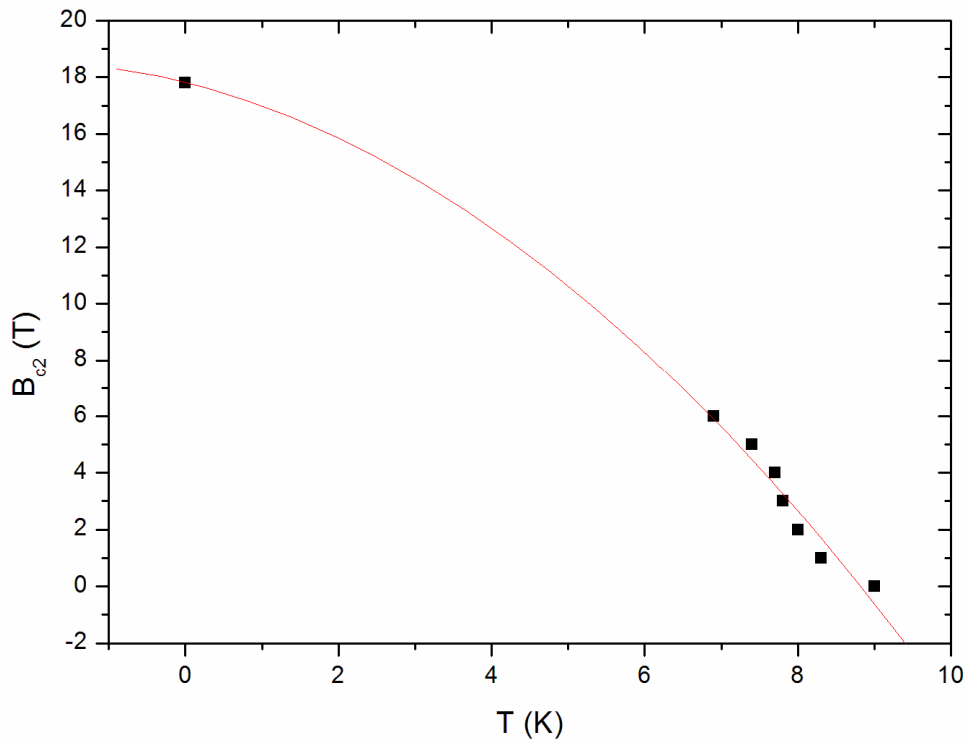


Figure 9. H_{c2} versus temperature extracted from resistivity measurements which show good agreement with WHH model (red line).

Bulk superconductivity is demonstrated by the heat capacity measurement shown in Figure 10. A clear jump is observed in C/T plotted against T^2 at zero magnetic field and the critical temperature is consistent in both resistivity and magnetization measurements. The normal state fit to the expression $C_n = \gamma T + \beta T^3$ by a least-squares analysis yields the values $\gamma = 3.8$ (mJ/molK²) and $\beta = 0.034$ (mJ/molK⁴). This result shows unambiguously that $Zr_{0.96}V_{0.04}B_2$ is a bulk superconductor. The subtraction of the phonon contribution allows us to evaluate the electronic contribution to the specific-heat, plotted as C_e/T vs T in the inset of figure 10.

An analysis of the jump yields $\Delta C_e/\gamma_n T_c \sim 0.49$ which is about 45% of the 1.43 value that is weak-coupling BCS prediction. This superconducting fraction is consistent with the estimative of fraction revealed by magnetization measurements displayed in Figure 6. Thus, these results show unambiguously that the substitution of Zr for V in the matrix ZrB_2 is able to induce bulk superconductivity in a matrix that is not a superconductor.

When this sample is annealed at 2000°C for 24 hours, the superconducting behavior disappears. This result strongly suggests that the original samples produced by arc-melting produce a supersaturated solution with V that does not exist in thermodynamic equilibrium. This supersaturation is close to a structural instability which probably is responsible for the superconducting behavior found in all as-cast samples. This interpretation provides an example of superconductivity that can emerge in the vicinity of some instability such as in A15 materials or other examples presented in introduction to this chapter.

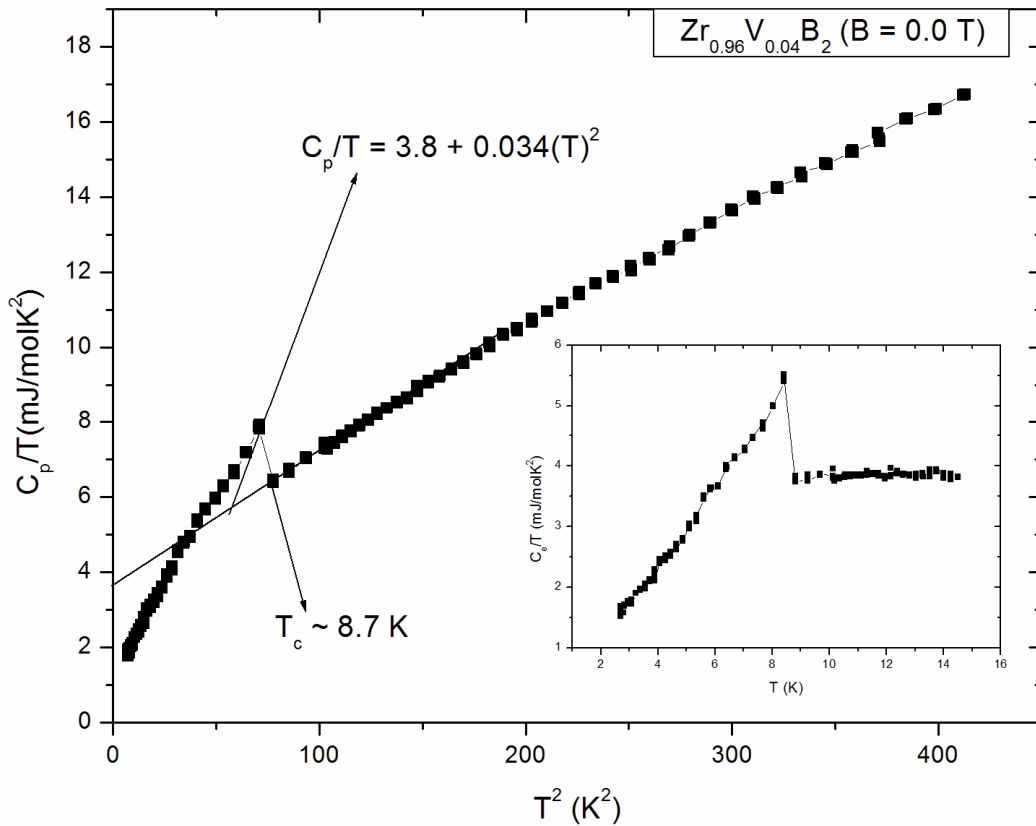


Figure 10. C_p/T against T^2 showing the clear jump close to the superconducting transition. The inset is shows the electronic contribution to the specific-heat.

1.1.2. Superconductivity in quasi-1D systems

During the last years great attention has been given to the study of superconductivity in low-dimensional (D) systems. This was motivated by the discovery of highly anisotropic behavior in high critical temperature cuprate and pnictide superconductors [22-24]. 1D systems are interesting because they are supposed to be simpler than 2D and 3D systems with regard to the electrical transport mechanisms. They offer a possibility to be compared with theoretical models for 1D conductors such as Luttinger Liquid (LL) theory [25,26] and Charge Density Wave (CDW) transition [6,7].

Generally, CDW transition exists in 1D systems as a consequence of the Peierls instability which is marked by the metal–insulator transition seen in electrical resistivity curves as a function of temperature [27]. One good example is the $\text{K}_{0.3}\text{MoO}_3$ compound [28]. On the other hand, LL behavior has been found only in special cases [29-30]. The best example recognized nowadays for the LL physics is the $\text{Li}_{0.9}\text{Mo}_6\text{O}_{17}$ purple bronze compound [31,32]. The electrical resistance behavior of this compound is well described by two power law temperature terms. The origin of the 1D electrical behavior of this compound is associated with Mo-O-Mo channels running along the b-axis of the monoclinic structure (for a good view of the crystalline structure see Fig. 2 of the reference [33]). The 1D behavior observed in the compound has been associated with the superconductivity

with $T_c = 1.9$ K [34]. Furthermore, the 1D electrical conductivity, the charge hopping between 1D channels, the observation of Bose metal in the superconducting state, and the suppression of the metal-insulator transition at 25 K with increasing hydrostatic pressure along with consequent increasing of the superconducting critical temperature has been carefully discussed [31,34]. This has led to a new discussion concerning whether the correlation between 1D behavior and superconductivity could exist in other compounds.

Based upon those observations in the purple bronze compound, our group has directed attention to the search for superconductivity in other molybdate oxides with low-D electrical conductivity. One example is the $A_x\text{MoO}_{2-\delta}$ compound with $A = \text{K}$ or Na and $x \leq 0.3$. Samples of this compound were prepared by solid state diffusion reaction using Mo , MoO_3 , K_2MoO_4 , and Na_2MoO_4 in appropriate amounts, encapsulated in quartz tube under vacuum or argon atmosphere, and heat treated at 400°C for 24 h followed by 700°C for 72 h. X-ray powder diffractometry showed that the samples are single phase and can be indexed with monoclinic structure of the space group $P2_1/c$ (14) and lattice parameters $a = 5.62$, $b = 4.85$, $c = 5.63$ Å, and $\beta = 120.92^\circ$. The crystalline structure of the compound is shown in Fig. 12.

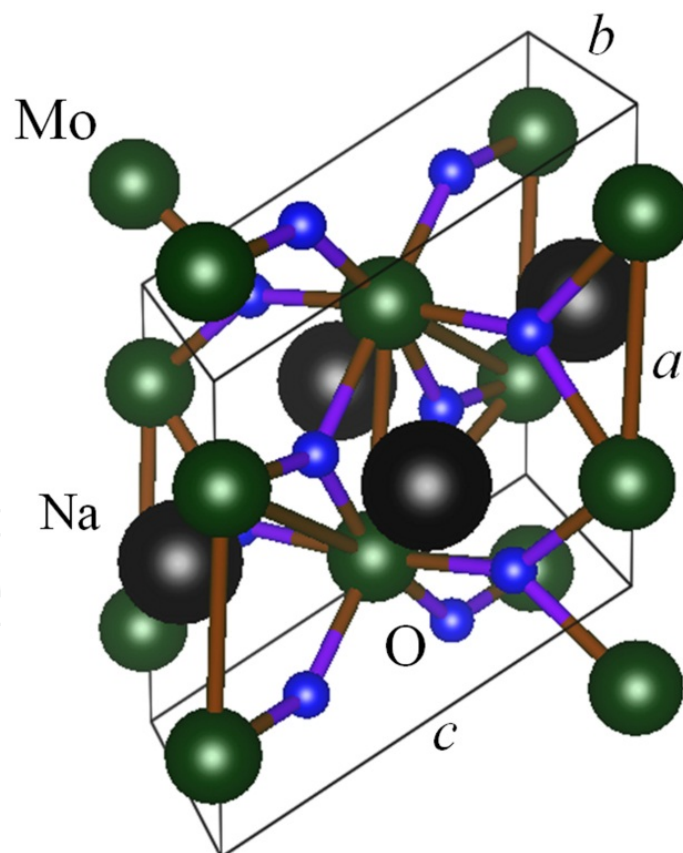


Figure 11. Crystalline structure of the $A_x\text{MoO}_{2-\delta}$ with $A = \text{Na}$ or K .

1D channels of Mo-O-Mo run along a-axis which is responsible for the anisotropic electrical behavior of this compound. In fact, samples with $A = \text{Na}$ and/or K show anomalous metallic

behavior at low temperatures. Figure 13 displays the electrical resistance as a function of temperature for the Na_{0.2}MoO_{2- δ} samples.

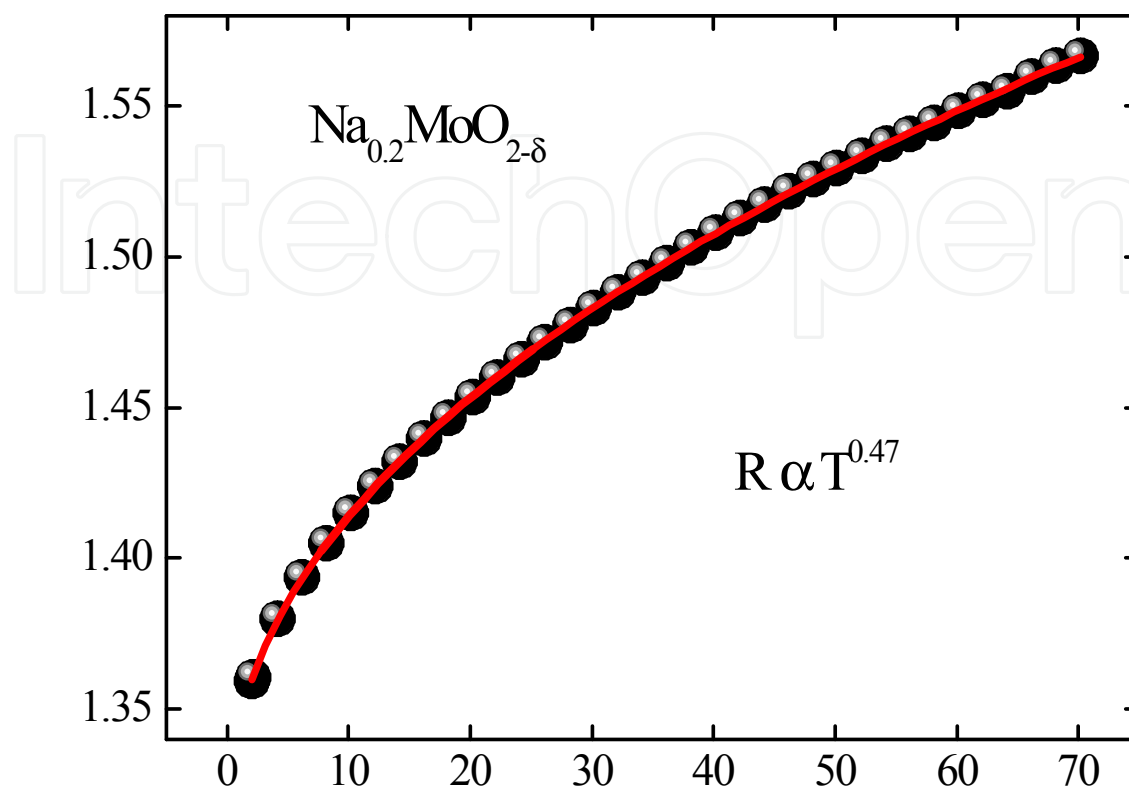


Figure 12. Typical anomalous electrical behavior observed in the Na_{0.2}MoO_{2- δ} compound.

A clearly anomalous non-linear behavior can be seen below 70 K. The electrical behavior can be well fit based upon the LL theory [4,5] using a single power law temperature term, $R \sim T^n$ with $n = 0.468 \pm 0.002$ which is closed to the value expected in the LL theory ($n = 0.5$) [35]. The excellent quality of the fit suggests that the compound shows a quasi-1D electrical conductivity. All the samples studied in the (Na,K)_xMoO_{2- δ} system show similar power law temperature dependence below 70 K.

One of the most interesting aspects associated with this anomalous behavior is the existence of superconductivity in some samples. Figure 14 shows the magnetization as a function of temperature measured in the zero field cooled (ZFC) and field cooled (FC) condition in the K_{0.05}MoO_{2- δ} sample.

A superconducting temperature can be clearly observed at $T_c = 4$ K in the sample. Furthermore, a magnetic ordering is noticed at $T_M = 65$ K. The coexistence of the anomalous behavior, magnetic ordering, and superconductivity are common effects observed in several samples of A_xMoO_{2- δ} system. The correlation between the quasi-1D conductivity, superconductivity, and weak ferromagnetism is still under investigation [35-38].

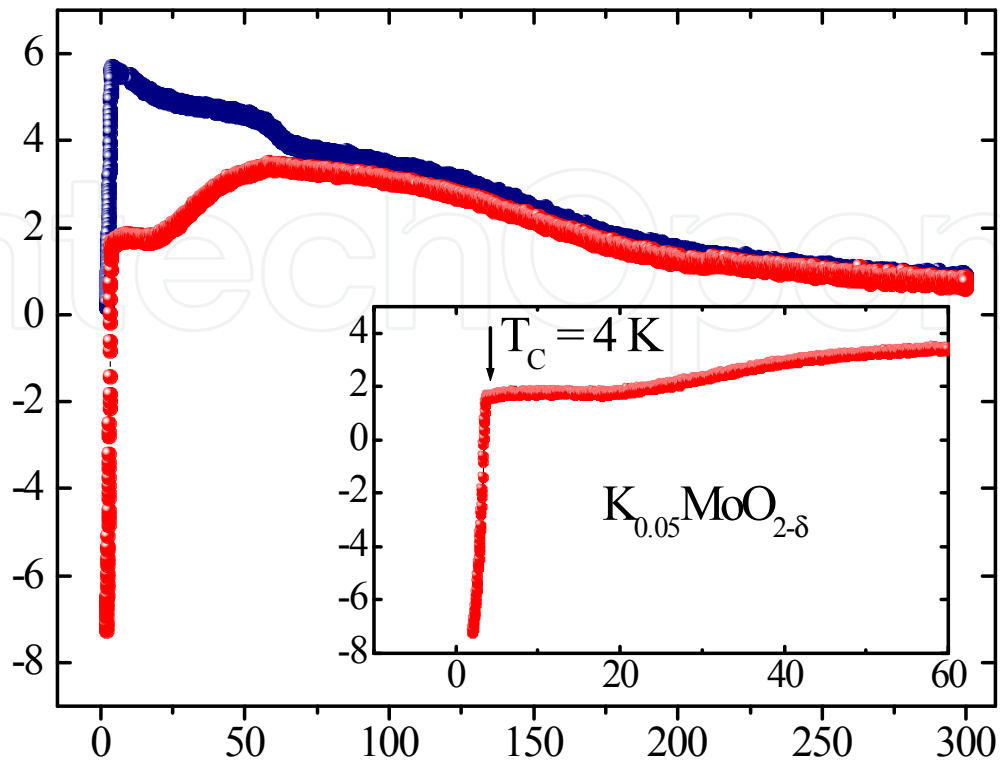


Figure 13. Magnetization as a function of temperature measured in the ZFC and FC procedures measured in the $\text{K}_{0.05}\text{MoO}_{2-\delta}$ sample.

2. Conclusions

This chapter reported the influence of the defects in the crystalline structure on the superconducting properties of intermetallic and low-dimensional compounds. The superconducting critical temperature of the materials can be associated with the electronic properties of the normal state. CDW, SDW, anisotropic behavior, structural phase transition, and doping content play important role on the superconducting properties of the compounds. Results about the influence of the crystalline structure on the superconducting properties for the MeB_2 and $\text{A}_x\text{MoO}_{2-\delta}$ compounds have been reported.

Author details

A.J.S. Machado, S.T. Renosto, C.A.M. dos Santos and L.M.S. Alves
Escola de Engenharia de Lorena, Universidade de São Paulo, Lorena, SP, Brazil

Z. Fisk
*Departments of Physics and Astronomy,
 University of California at Irvine, Irvine, USA*

Acknowledgement

The authors are grateful by financial support through of the following grants (CNPq Brazilian Agency grant n° 303813/2008-3, 490182/2009-7 and 309084/2010-5) (Fapesp Brazilian Agency grant n° 2011/05961-3, 2009/54001-2, 2009/14524-6, 2010/06637-2 and 2010/11770-3) and AFOSR MURI.

3. References

- [1] Bardeen, J.; Cooper, L. N.; Schrieffer, J. R. *Phys. Rev.*, 108 (1957) 1175.
- [2] C. W. Chu and L. R. Testardi, *Phys. Rev. Lett.*, 32 (1974) 766.
- [3] Z. Fisk, H. R. Ott and J. D. Thompson, *Philosoph. Magazine*, 89 (2009) 2111.
- [4] C. Escribe-Filippini, J. Beille, M. Boujida, and C. Schlenker, *Phys. C*, 427 (1989)162.
- [5] C. A. M. dos Santos, M. S. da Luz, Yi-Kuo Yu, J. J. Neumeier, J. Moreno, and B. D. White, *Phys. Rev. B* 77 (2008) 193106.
- [6] A. S. Cooper, E. Corenzwit, L. D. Longinotti, B. T. Matthias and W. H. Zachariasen, *Proceedings of the National Academy of Sciences*, 67 (1970) 313.
- [7] Nagamatsu J, Nakagawa N., Murakana Y. Z., Akimitsu J., *Nature*, 410, (2001), 63-64.
- [8] Carlos Angelo Nunes, Dariusz Kaczorowski, Peter Rogle, Marica Regina Baldissera, Paulo Atsushi Suzuki, Gilberto Carvalho Coelho, Andriy Grytsiv, Gilles André, Françoise Bouree, Shigeru Okada, *Acta Materialia*, 53, (2005), 3679.
- [9] T. Massalski. H. Okomono, P. Subramanian, L. Kacprozak (Eds), *Binary Alloy Phase Diagrams*, 2 and Edition American Society For Metals, Metals Park, 1990.
- [10] Meerson G. A., Samsonov G. V., *J. Chem. USSR*, 27, (1954), 1053.
- [11] L. E. Muzzy, M. Avdeev, G. Lawes, M. K. Haas, H. W. Zandbergen, A. P. Ramirez, J. D. Jorgensen, R. J. Cava, *Physica C*, 382 (2002) 153.
- [12] S. Sanfilippo, H. Elsinger, M. Núñez-Regueiro and O. Laborde, *Phys. Rev. B*, 61 (2000) R3800.
- [13] A. L. Ivanovskiĭ, *Usp. Khim.* 70 (9), 811 (2001).
- [14] J. Kortus, I. I. Mazin, K. D. Belaschenko, *et al.*, *Phys. Rev. Lett.* 86 (20), 4656 (2001).
- [15] J. M. An and W. E. Pickett, *Phys. Rev. Lett.* 86 (19), 4366 (2001).
- [16] N. I. Medvedeva, A. L. Ivanovskii, J. E. Medvedeva, and A. J. Freeman, *Phys. Rev. B* 64, 020502 (2001).
- [17] I. R. Shein, and A. L. Ivanovskii, *Phys. Sol. State*, vol. 44, N.10, 1833-1839 (2002).
- [18] V. A. Gasparov, N. S. Sidorov, I. L. Zver'kova, and M. P. Kulakov, *Pis'ma Zh. Éksp. Teor. Fiz.* 73 (10), 601 (2001) [*JETP Lett.* 73, 532 (2001)].
- [19] V. A. Gasparov, N. S. Sidorov and I. I. Zver'kova, *Physical Review B*, 73, 094510 (2006).
- [20] Z. Fisk, A.C. Lawson, B.T. Matthias, E. Corenzwit, *Phys. Lett. A* 37, 251 (1971).
- [21] A.S. Pereira, C.A. Perottoni, J.A.H. da Jornada, J.M. Leger, J. Haines, *J. Phys. Cond. Mat.*, 14, 10615 (2002).
- [22] N. R. Werthamer; E. Helfand; and P. C. Hohenberg, *Phys. Rev.*, 147 (1966) 295.
- [23] S. W. Tozer, A. W. Kleinsasser, T. Penney, D. Kaiser, and F. Holtzber, *Phys. Rev. Lett.* 59, 1768 (1987).

- [24] M. A. Tanatar, N. Ni, C. Martin, R. T. Gordon, H. Kim, V. G. Kogan, G. D. Samolyuk, S. L. Bud'ko, P. C. Canfield, and R. Prozorov, *Phys. Rev. B* 79, 094507 (2009).
- [25] V. N. Zavaritsky and A. S. Alexandrov, *Phys. Rev. B* 71, 012502 (2005).
- [26] J. Voit, *Rep. Prog. Phys.* 58, 977 (1995).
- [27] M. Ogata and P. W. Anderson, *Phys. Rev. Lett.* 70, 3087 (1993).
- [28] W. L. McMillan, *Phys. Rev. B* 14, 1496 (1976).
- [29] A. Berlinsky, *Rep. Prog. Phys.* 42, 1243 (1979).
- [30] R. E. Thorne, *Phys. Today*, 42 (1996).
- [31] R. Tarkiainen, M. Ahlskog, J. Penttilä, L. Roschier, P. Hakonen, M. Paalanen, and E. Sonin, *Phys. Rev. B* 64, 195412 (2001).
- [32] S. N. Artemenko and S. V. Remizov, *Phys. Rev. B* 72, 125118 (2005).
- [33] C. A. M. dos Santos, M. S. da Luz, Yi-Kuo Yu, J. J. Neumeier, J. Moreno, and B. D. White, *Phys. Rev. B* 77, 193106 (2008).
- [34] C. A. M. dos Santos, B. D. White, Yi-Kuo Yu, J. J. Neumeier, and J. A. Souza, *Phys. Rev. Lett.* 98, 266405 (2007).
- [35] M. S. da Luz, J. J. Neumeier, C. A. M. dos Santos, B. D. White, H. J. Izario Filho, J. B. Leão, and Q. Huang, *Phys. Rev. B* 84, 014108 (2011).
- [36] C. Escribe-Filippini, J. Beille, M. Boujida, and C. Schlenker, *Physica C* 162-164, 427 (1989).
- [37] L. M. S. Alves, V. I. Damasceno, C. A. M. dos Santos, A. D. Bortolozo, P. A. Suzuki, H. J. Izario Filho, A. J. S. Machado, and Z. Fisk, *Phys. Rev. B* 81, 174532 (2010).
- [38] L. M. S. Alves, C. A. M. dos Santos, S. S. Benaion, A. J. S. Machado, B. S. de Lima, J. J. Neumeier, M. D. R. Marques, J. A. Aguiar, R. J. O. Mossaneck, and M. Abbate. Submitted to *Phys. Rev. B* (2012).